

# The Concentration Effects for the Adsorption Behavior of Heptyl Viologen Cation Radicals on Indium-Tin-Oxide Electrode Surfaces

Yusuke Ayato, Takashi Itahashi, Akiko Takatsu, Kenji Kato, and Naoki Matsuda<sup>†</sup>

**Abstract**—In situ observation of absorption spectral change of heptyl viologen cation radical ( $HV^{+•}$ ) was performed by slab optical waveguide (SOWG) spectroscopy utilizing indium-tin-oxide (ITO) electrodes. Synchronizing with electrochemical techniques, we observed the adsorption process of  $HV^{+•}$  on the ITO electrode. In this study, we carried out the ITO-SOWG observations using KBr aqueous solution containing different concentration of HV to investigate the concentration dependent spectral change. A few specific absorption bands, which indicated  $HV^{+•}$  existed as both monomer and dimer on ITO electrode surface with a monolayer or a few layers deposition, were observed in UV-visible region. The change in the peak position of the absorption spectra from adsorption species of  $HV^{+•}$  were correlated with the concentration of HV as well as the electrode potential.

**Keywords**—absorption phenomena, heptyl viologen, indium-tin-oxide (ITO) electrode, in situ, slab optical waveguide (SOWG) spectroscopy,

## I. INTRODUCTION

WE have been studying the adsorption process and adsorbed states of various molecules on solid/liquid interfaces by slab optical waveguide (SOWG) spectroscopy [1]-[7]. Our recent improvement of the SOWG instrument based on the light incidence method utilizing a glycerol drop has enabled us to observe time dependent adsorption behavior [8]-[11], and to obtain the standard Gibbs free energy ( $\Delta G$ ) value due to adsorption process of proteins on solid/liquid interfaces. The development of an indium-tin-oxide (ITO) coated SOWG (ITO-SOWG) has also allowed us to carry out the spectroelectrochemical observation of adsorbed molecules accompanied by redox reaction at electrochemical interfaces [12]-[14].

N,N'-Disubstituted-4,4'-bipyridinium salts (viologens) were first studied for electrochromic devices (ECDs) in 1970s

Y. Ayato and N. Matsuda<sup>†</sup> are with On-site Sensing and Diagnosis Research Laboratory, AIST, 807-1, Shuku, Tosu, Saga, 841-0052, Japan (corresponding author<sup>†</sup> to provide phone: +81-942-81-3623; fax: +81-942-81-3690; e-mail: naoki.matsuda@aist.go.jp).

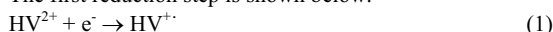
T. Itahashi is with Mechanical and Electrical Systems Engineering Advanced Course, Kurume National College of Technology, 1-1-1, Komorino, Kurume, Fukuoka, 830-8555, Japan.

A. Takatsu and K. Kato are with National Metrology Institute of Japan, AIST, Central 3, 1-1-1, Umezono, Tsukuba, 305-8563, Japan.

and have been attracted much attention for the application owing to their high transmittance changes and fast responses [15]-[17]. Recent studies have been performed for applications of viologens to herbicides, electron mediators and catalysts [18]-[20]. 1,1'-Dimethyl-4,4'-bipyridinium (methyl viologen ; MV) modified electrodes exhibit measurable rates of heterogeneous electron transfer with several biological molecules [21], [22]. 1,1'-Diheptyl-4,4'-bipyridinium (heptyl viologen ; HV) is usually studied for electrochromic applications because its one-electron reduction of the dication  $HV^{2+}$  to the mono-cation radical salt  $HV^{+•}$  in aqueous solutions can form a precipitate with violet color on electrode surfaces [23]-[32].

$HV^{2+}$  has been known to receive two-step one-electron reactions resulting in the formation of  $HV^{+•}$  and HV.

The first reduction step is shown below.



It is reversible reaction and immediately follows chemical reaction with proper counter anions ( $X^{-}$ ), which produced a cation radical salt film on electrodes with strong violet color. Jasinski reported that the precipitates film of  $HV^{+•}X^{-}$  has amorphous structure in the primary stage of the film formation process, then, the phase gently and unsteadily changes in successive reactions, and the aging process follows [33].

The second reduction step of  $HV^{+•}$  can be expressed by Eq. (2):



It is less reversible reaction and forms a solid deposit with yellow color on the electrode surface. These film formation processes have been solved by a number of researchers using various analytic techniques [31], [34]-[38]. However, so little report included the time and the potential dependent adsorption states change on the electrode surfaces covered with the monolayer or a few layers deposition.

Although a number of researchers have demonstrated for the reduction process of the first reduction step of  $HV^{2+}$ , they mainly observed the adsorption states of  $HV^{+•}$  in multilayer deposition on the electrode surface. In addition, they usually discussed the behavior of the absorption bands at around 550 nm, so little reports included the results of the absorption bands at around 400 nm. The information of the absorption band only at around 550 nm is insufficient to comprehend the potential

dependent adsorption process of  $HV^{2+}$  on the electrode surface, because the absorption bands of  $HV^{2+}$  monomer and dimer are observed in one broad band consisting of a few absorption bands.

The main aim of present study is to discuss the adsorption behavior of  $HV^{2+}$  monomer and dimer, especially in a monolayer deposition, separately by employing the absorption bands at around 400 nm. And we will note and investigate the potential dependent adsorption behavior of  $HV^{2+}$  molecules by the spectroelectrochemical SOWG using different concentration of  $HV$ .

## II. EXPERIMENTALS

### A. Materials

Heptylvologen dibromide ( $HVBr_2$ ) purchased from Tokyo Kasei Industry Co., Ltd. was used as received without further purification. Potassium bromide (KBr) used as the supporting electrolyte was guaranteed grade and purchased from Kanto Chemical Co., Inc. The sample solutions were prepared using Milli-Q water (resistivity  $> 18 M\Omega cm$ ). The concentrations of  $HVBr_2$  were adjusted to  $1 \times 10^{-3}$ ,  $5 \times 10^{-5}$  and  $1.25 \times 10^{-5} mol dm^{-3}$  and that of KBr was  $0.3 mol dm^{-3}$ .

### B. Spectroelectrochemical SOWG Systems

The experimental details of SOWG have been given elsewhere [11], [13], [39]. As shown in Fig. 1, a 150-W xenon lamp (System Instruments Co., Ltd., Japan) was used as the light source, and the light was guided by an optical fiber. The SOWG spectra were detected using a CCD detector with monochromator (PMA-11, Hamamatsu Photonics, Japan). The minimum time resolution of the CCD detector is 20 ms. The ITO film was formed by vapor deposition on a glass plate ( $50 mm \times 20 mm \times 0.05 mm$ , Matsunami Glass Industry, Ltd., Japan) giving a thickness of approximately 20 nm. ITO-SOWG plates were cleaned by soaking in ethanol for 1 h and then rinsed extensively with Milli-Q water. The spectroelectrochemical surface area of ITO-SOWG working electrode covered with sample solution was approximately  $1.3 cm^2$ . A platinum wire and an  $Ag/AgCl$  electrode were used as the counter and reference electrodes, respectively. All the potentials in this paper are quoted against  $Ag/AgCl$ . The electrode potential was controlled with a potentiostat (EG&G Princeton Applied Research, Model 273) synchronizing with the spectrometer.

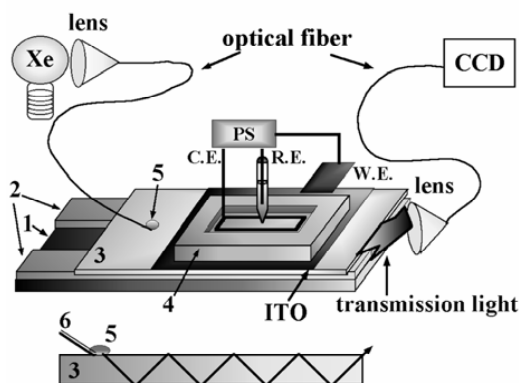


Fig. 1 Illustration of ITO-SOWG systems. 1: slide glass base, 2: silicon rubber strip acting SOWG supports, 3: SOWG ( $50 \times 20 \times 0.05 mm$ ), 4: leak-proof silicone rubber solution cell, 5: glycerol drop, and 6: optical fiber from the light source. PS: Potentiostat, W.E., C.E., and R.E.: working (ITO), counter (Pt wire), and reference ( $Ag/AgCl$ ) electrode, and ITO: indium-tin-oxide electrode.

### C. Measurements

The resulting SOWG spectra are shown in terms of absorbance units defined as follows:

$$A = -\log(I_S/I_R) \quad (3)$$

Where  $I_S/I_R$  represent the relative change in the intensity and  $I_S$  and  $I_R$  are the sample and reference intensities, respectively. All reference spectra on the SOWG analysis were observed at  $-200 mV$  in this study.

In situ spectroelectrochemical SOWG observations were carried out with synchronized with cyclic voltammetric measurements. The electrode potential was swept to the cathodic direction from  $-200$  to  $-600 mV$ , and back to  $-200 mV$  at a sweep rate of  $10 mV s^{-1}$ . The time width of each spectrum was 600 ms and SOWG spectra were obtained continuously.

A potential step method was also applied to in situ SOWG measurements. Before the sample measurements, the electrode potential was held at  $-200 mV$  for 30 s and the reference spectrum was measured with the exposure time of 300 ms. The resulting spectra were measured at  $-600 mV$  for 60 s with the exposure time of 300 ms.

## III. RESURUTS AND DISCUSSION

### A. Cyclic voltammetry

The first one-electron reduction of  $HV^{2+}$  giving the radical salt is known to a simple, soluble and reversible reaction. Since the electron transfer reaction is fast, it is effectively diffusion controlled at enough large current densities [40]. Fig. 2 shows the cyclic voltammogram measured in  $0.3 mol dm^{-3}$  KBr aqueous solution containing  $1 \times 10^{-3} mol dm^{-3} HV^{2+}$ . A pair of the peaks was observed at around  $-400$  and  $-500 mV$ . One peak at around  $-500 mV$  corresponds to the one-electron reduction shown in Eq. (1), and another peak at around  $-400 mV$  indicates

the oxidation from  $HV^{+}$  to  $HV^{2+}$ , which is the reversal reaction of Eq. (1). A strong violet color was observed directly by eyes from the precipitates film was formed on the electrode surface below  $-500$  mV.

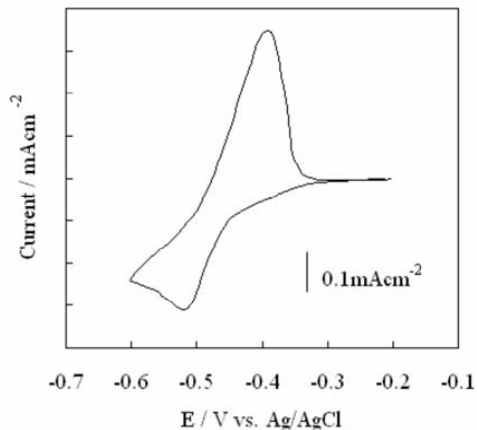


Fig. 2 Cyclic voltammograms at ITO electrodes for  $1 \times 10^{-3}$  mol  $dm^{-3}$   $HVBr_2$  in  $0.3$  mol  $dm^{-3}$  KBr aqueous solution. Sweep rate:  $100$  mV  $s^{-1}$ .

The surface coverage of the electrode can be estimated from the redox current of the cyclic voltammograms. The charge density in  $1 \times 10^{-3}$  mol  $dm^{-3}$   $HV^{2+}$  containing solution was approximately  $140$   $\mu C$   $cm^{-2}$ . The charge density for the reduction of  $HV^{+}$  of monolayer coverage, assuming one molecule occupies  $0.5$  or  $1$   $nm^2$ , is about  $32$  or  $16$   $\mu C$   $cm^{-2}$ . Thus, the electrode surface should be covered with multilayer precipitates film of  $HV^{+}$ . To investigate the change in the adsorption states of  $HV^{+}$  molecules in a thin deposition layer, we carried out the cyclic voltammetric measurements with following experimental condition. The electrode potential was held at  $-600$  mV for  $60$  s in  $0.3$  mol  $dm^{-3}$  KBr aqueous solution containing  $5 \times 10^{-5}$  mol  $dm^{-3}$   $HV^{2+}$ , and then swept at  $20$  mV  $s^{-1}$  from  $-600$  to  $-200$  mV. The charge density was obtained approximately  $40$   $\mu C$   $cm^{-2}$  from the first cycle of the cyclic voltammograms. Thus, all spectroelectrochemical SOWG data obtained in this study should be based on the potential dependent change of adsorbed  $HV^{+}$  molecules in the monolayer or a few deposition layers on the electrode surface.

#### B. In Situ Spectroelectrochemical Observations by SOWG Spectroscopy Synchronizing with Cyclic Voltammetric Measurements

Fig. 3 shows SOWG absorption spectra obtained by synchronizing with cyclic voltammetric measurements using  $0.3$  mol  $dm^{-3}$  KBr aqueous solution containing  $5 \times 10^{-5}$  mol  $dm^{-3}$   $HV^{2+}$ . It has been known that several absorption bands assigned to  $HV^{+}$  species are observed in UV-visible region [41]. As shown in the Fig. 3, several positive-going bands were observed at around  $400$  and  $550$  nm. The absorption band at around  $380$  nm, which was assigned to the dimer of  $HV^{+}$  [41],

appeared in UV-visible region below about  $-400$  mV ( $20$  s) and another absorption at around  $400$  nm, which was assigned to a monomer of  $HV^{+}$  [41], seems to arise from more positive electrode potential. The absorption band at around  $530$  nm appeared as a broad-band below about  $-400$  mV, which was assigned to dimer of  $HV^{+}$  [42]. The absorption band at around  $550$  nm might be observed due to the different aggregation from monomer and dimer of  $HV^{+}$  [43].

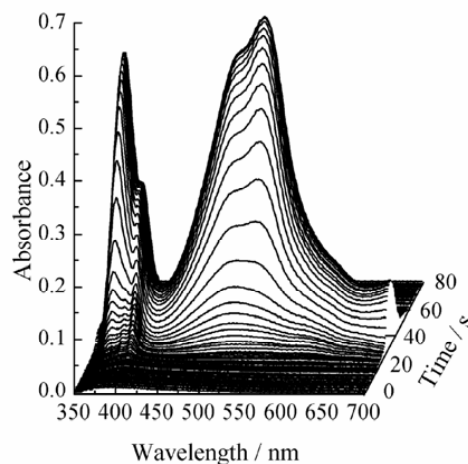


Fig. 3 Time-resolved SOWG spectra synchronized with cyclic voltammetric measurements in  $0.3$  mol  $dm^{-3}$  KBr aqueous solution containing  $5 \times 10^{-5}$  mol  $dm^{-3}$   $HV$ . Sweep rate:  $10$  mV  $s^{-1}$ .

Fig. 4 shows the potential dependent change in the intensity and peak position of the absorption bands at around  $380$  and  $400$  nm obtained by SOWG data synchronized with cyclic voltammetric measurements. The intensities of adsorption bands at around  $400$  and  $380$  nm started to increase monotonically with decreasing the electrode potential at around  $16.8$  and  $21$  s passed (at  $-368$  and  $-410$  mV). Contrary to the results for the cathodic polarization, the intensities of them decreased with increasing the electrode potential and disappeared completely at around  $63.6$  and  $60.6$  s ( $-364$  and  $-394$  mV) in the anodic polarization. Thus, it was confirmed that the dimer of  $HV^{+}$  adsorbed at lower electrode potential region than the monomer of  $HV^{+}$  on the electrode surface.

In the potential dependent peak position change, the band at around  $400$  nm showed no peak shift of absorption band under this experimental condition, as shown in Fig. 4(a). This result was very similar to that observed in our former study [41]. On the other hand, the peak position at around  $380$  nm has been known to show the peak shifts depended on the electrode potential [41]. The absorption band at around  $380$  nm appeared at  $374$  nm and exhibited a red shift to  $380$  nm with decreasing electrode potential. In the positive polarization, a blue shift of the maximum absorption wavelength was observed from  $380$  to  $374$  nm. These results were also similar to those observed in our former study [41]. The peak shift of the absorption band at

around 380 nm implied that the different aggregation of  $HV^{2+}$  adsorbed on the electrode surface.

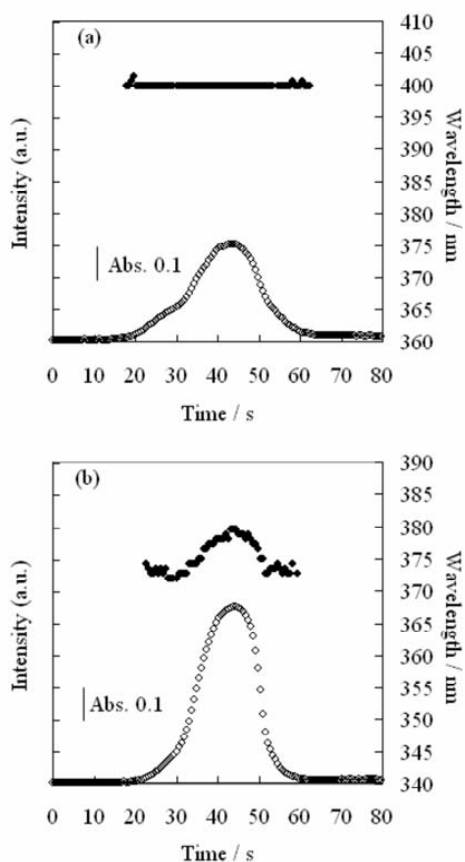


Fig. 4 Change in the intensity and peak position at around 400 nm (a) and 380 nm (b) obtained from time-resolved SOWG analysis synchronized with cyclic voltammetric measurements in  $0.3 \text{ mol dm}^{-3}$  KBr aqueous solution containing  $5 \times 10^{-5} \text{ mol dm}^{-3}$  HV. Sweep rate:  $10 \text{ mV s}^{-1}$ .

#### C. In Situ SOWG Measurements using Potential Step Methods

To investigate whether the absorption band at around 380 nm shows the peak shift depending on the concentration of HV or not, we carried out time-resolved SOWG observations by synchronizing with potential step measurements in  $0.3 \text{ mol dm}^{-3}$  KBr aqueous solutions containing 5 and  $1.25 \times 10^{-5} \text{ mol dm}^{-3}$   $HV^{2+}$ . Fig. 5 shows the change in the peak position of absorption band at around 380 nm obtained by SOWG analysis synchronizing with potential step measurements from -0.2 to -0.6 V for 60 s. In potential step measurements, the peak position of the absorption band at around 380 nm exhibited a red shift from around 375 to 390 nm from 0.3 to 60 s in  $5 \times 10^{-5} \text{ mol dm}^{-3}$   $HV^{2+}$  containing solution. On the other hand, clear peak shift of the absorption band at 380 nm was not observed

for 60 s in the case of using  $1.25 \times 10^{-5} \text{ mol dm}^{-3}$   $HV^{2+}$  containing solution. These results indicate that the change in the peak position of the absorption band at around 380 nm probably depended on the concentration of HV as well as the electrode potential.

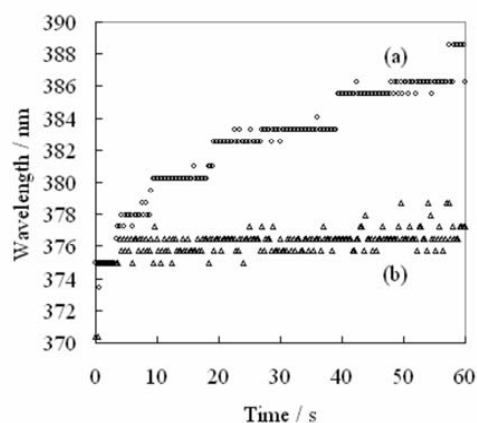


Fig. 5 Potential dependence of the peak position at around 380 nm obtained from time-resolved SOWG analysis synchronized with potential step measurements from -200 to -600 mV for 60 s in  $0.3 \text{ mol dm}^{-3}$  KBr aqueous solutions containing 5 (a) and  $1.25 \times 10^{-5}$  (b)  $\text{mol dm}^{-3}$  HV.

Consequently, we carried out a very successful observation for the heptilviologen cation radicals on the electrode surface by using spectroelectrochemical SOWG. The adsorption behavior of  $HV^{2+}$  could be clearly characterized and distinguished both monomer and dimer by employing the absorption bands at around 400 nm.

This technique we have presented allowed the very successful observation of both the spectroscopic and electrochemical properties of molecules on electrode/electrolyte interfaces. Highly sensitive in situ SOWG spectra yield essential molecular information for coverage of monolayer or a few layers.

#### IV. CONCLUSION

The ITO-SOWG successfully observed the potential and concentration dependent structural changes. It was found from SOWG studies that several different species of  $HV^{2+}$  adsorbed on the electrode surface. The dimer of  $HV^{2+}$  was adsorbed more negative electrode potential than the monomer of  $HV^{2+}$  on the ITO electrode surfaces. These monomeric and dimeric  $HV^{2+}$  molecules co-adsorbed on the ITO electrode surface in all applied negative electrode potential region. The adsorption states of  $HV^{2+}$  molecules depended on the concentration of HV as well as the electrode potential.

We presented an application of the SOWG spectroscopy, which can easily and directly yield in situ molecular information on electrode/electrolyte interfaces. This powerful technique will disclose the configurations of many other

molecules adsorbed on the electrode surfaces.

## REFERENCES

- [1] K. Kato, A. Ataka, N. Matsuda and Y. Sugitani. *Chem. Lett.*, **1997**, p. 583, 1997.
- [2] K. Kato, A. Takatsu and N. Matsuda. *Chem. Lett.*, **1999**, p. 31, 1999.
- [3] J. H. Santos, N. Matsuda, Z. Qi, A. Takatsu and K. Kato. *Anal. Sci.*, **19**, p. 199, 2003.
- [4] K. Ito and A. Fujishima. *J. Phys. Chem.*, **92**, p. 7043, 1988.
- [5] K. Tsunoda, T. Umemura, H. Ueno, E. Okuno and H. Akaiwa. *Appl. Spectrosc.*, **57**, p. 1273, 2003.
- [6] D. R. Dunphy, S. B. Mendes, S. S. Saavedra and N. R. Armstrong. *Anal. Chem.*, **69**, p. 3086, 1997.
- [7] K. Fujita and H. Ohno. *Polym. Advanced Technol.*, **14**, p. 486, 2003.
- [8] Z.-M. Qi, N. Matsuda, A. Takatsu and K. Kato. *J. Phys. Chem. B*, **107**, p. 6873, 2003.
- [9] J. H. Santos, N. Matsuda, Z.-M. Qi, T. Yoshida, A. Takatsu and K. Kato. *Mater. Trans.*, **45**, p. 1015, 2004.
- [10] Z.-M. Qi, N. Matsuda, A. Takatsu and K. Kato. *Langmuir*, **20**, p. 778, 2004.
- [11] Z.-M. Qi, N. Matsuda, T. Yoshida, H. Asano, A. Takatsu and K. Kato. *Opt. Lett.*, **15**, p. 2001, 2002.
- [12] N. Matsuda, A. Takatsu, K. Kato and Y. Shigesato. *Chem. Lett.*, **1998**, p. 125, 1998.
- [13] N. Matsuda, J. H. Santos, A. Takatsu and K. Kato. *Thin Solid Films*, **438-439**, p. 403, 2003.
- [14] N. Matsuda, J. H. Santos, A. Takatsu and K. Kato. *Thin Solid Films*, **445**, p. 313, 2003.
- [15] E. Kirowa-Eisner and E. Gileadi. *J. Electroanal. Chem.*, **25**, p. 481, 1970.
- [16] C. J. Schoot, J. J. Ponječ, H. T. van Dam, R. A. van Doorn and P. T. Bolwijn. *Appl. Phys. Lett.*, **23**, p. 64, 1973.
- [17] I. V. Shelepin, O. A. Ushakov, N. I. Karpova and V. A. Barachevskii. *Elektrokhimiya*, **13**, p. 32, 1977.
- [18] S. F. Bailey and L. M. Smith, "Handbook of Agricultural Pest Control", Industry Publications, New York, 1951.
- [19] T. Kuwana and E. Steckhan. *Ber. Bunsenges. Phys. Chem.*, **78**, p. 253, 1974.
- [20] A. I. Krasna. *J. Photochem. Photobiol.*, **31**, p. 75, 1980.
- [21] H. L. Landrum, R. T. Salmon and F. M. Hawkridge. *J. Am. Chem. Soc.*, **99**, p. 3154, 1977.
- [22] C. D. Crawley and F. M. Hawkridge. *Biochem. Biophys. Res. Commun.*, **99**, p. 516, 1981.
- [23] K. Arihara and F. Kitamura. *J. Electroanal. Chem.*, **550-551**, p. 149, 2003.
- [24] K.-C. Ho, Y.-W. Fang, Y.-C. Hsu and L.-C. Chen. *Solid State Ionics*, **165**, p. 279, 2003.
- [25] T. Sagara and K. Miuchi. *J. Electroanal. Chem.*, **567**, p. 193, 2004.
- [26] N. Leventis and Y. C. Chung. US patent 5,457,564, 1995.
- [27] J. Stepp and J. B. Schlenoff. *J. Electrochem. Soc.*, **144**, L155, 1997.
- [28] F. Campus, P. Bonhôte, M. Grätzel, S. Heinen and L. Walder. *Sol. Energy Mater. Sol. Cells*, **56**, p. 281, 1999.
- [29] T. Lu and T. M. Cotton. *J. Phys. Chem.*, **91**, p. 5978, 1987.
- [30] M. Osawa, K. Yoshii, Y. Hibino, T. Nakano and I. Noda. *J. Electroanal. Chem.*, **426**, p. 11, 1997.
- [31] Y. Misono, M. Nagase and K. Itoh. *Spectrochim. Acta*, **50A**, p. 1539, 1994.
- [32] K. Arihara and F. Kitamura. *J. Electroanal. Chem.*, **550-551**, p. 149, 2003.
- [33] R. J. Jasinski. *J. Electrochem. Soc.*, **124**, p. 637, 1977.
- [34] T. Kawata, M. Yamamoto, M. Yamana, M. Tajima and T. Nakano. *Jpn. J. Appl. Phys.*, **14**, p. 725, 1975.
- [35] A. Bewick, A. C. Lowe and C. W. Wederell. *Electrochim. Acta*, **28**, p. 1899, 1983.
- [36] M. Osawa and W. Suetaka. *J. Electroanal. Chem.*, **270**, p. 261, 1989.
- [37] T. M. Cotton, J.-H. Kim and R. A. Uphaus. *Microchem. J.*, **42**, p. 44, 1990.
- [38] H. X. Wang, T. Sagara, H. Sato and K. Niki. *J. Electroanal. Chem.*, **331**, p. 925, 1992.
- [39] J. H. Santos, N. Matsuda, Z.-M. Qi, T. Yoshida, A. Takatsu and K. Kato. *Surf. Interface Anal.*, **35**, p. 432, 2003.
- [40] M. Osawa, K. Yoshii, K. Ataka and T. Yotsuyanagi. *Langmuir*, **10**, p. 640, 1994.
- [41] Y. Ayato, A. Takatsu, K. Kato, J. H. Santos, T. Yoshida and N. Matsuda. *J. Electroanal. Chem.*, **578**, p. 137, 2005.
- [42] J. F. Stargardt and F. M. Hawkridge. *Anal. Chim. Acta*, **146**, p. 1, 1983.
- [43] Y. Ayato, A. Takatsu, K. Kato and N. Matsuda. *J. Electroanal. Chem.*, submitted.